Inkjet and 3D Printing Technology for Fundamental Millimeter-Wave Wireless Packaging

Bijan K. Tehrani, Ryan A. Bahr, and Manos M. Tentzeris
Georgia Institute of Technology | School of Electrical and Computer Engineering
85 5th St NW
Atlanta, GA 30308, USA
Ph: 770-289-6835
Email: btehrani3@gatech.edu

Abstract

This paper outlines the design, processing, and implementation of inkjet and 3D printing technologies for the development of fully-printed, highly-integrated millimeter-wave (mm-wave) wireless packages. The materials, tools, and processes of each technology are outlined and justified for their respective purposes. Inkjet-printed 3D interconnects directly interfacing a packaging substrate with an IC die are presented using printed dielectric ramps and coplanar waveguide (CPW) transmission lines exhibiting low loss (0.6–0.8 dB/mm at 40 GHz). Stereolithography (SLA) 3D printing is presented for the encapsulation of IC dies, enabling the application-specific integration of on-package structures, including dielectric lenses and frequency selective surface (FSS)-based wireless filters. Finally, inkjet and 3D printing technology are combined to present sloped mm-wave interconnects through an encapsulation, or through-mold vias (TMVs), achieving a slope up to 65° and low loss (0.5–0.6 dB/mm at 60 GHz). The combination of these additive techniques is highlighted for the development of scalable, application-specific wireless packages.

Key words

Millimeter-wave, packaging, interconnects, encapsulation, inkjet printing, 3D printing, stereolithography

I. Introduction

Growing trends in emerging wireless technologies are pushing for the realization of high-bandwidth data transmission and miniaturized form factor, along with a necessary reduction in fabrication cost. This next generation of mobile communication systems has highlighted the field of millimeter-wave (mm-wave) wireless technology, where carrier frequencies operate within the range of tens to hundreds of gigahertz. This increase in frequency from typical commercial microwave technologies allows for wider channel bandwidths, establishing interest in such fields as autonomous automotive radar, vehicle-to-vehicle (V2V) communication, and 5G gigabit wireless networks. Because of the reduction of wavelength throughout the mm-wave regime, packaging technology becomes especially important in the development of any practical wireless system. In order to miniaturize systems and reduce destructive high-frequency parasitics, the realization of system-on-package (SoP) packaging solutions is an area of popular research, where integrated circuit (IC) dies can be integrated directly with peripheral components, such as other ICs, antennas, and various other passive components required in any modern wireless system.

Three-dimensional (3D) first-level interconnects are required to interface an IC die with a packaging substrate and other electronic components within the same package. The two most standardized methods of realizing these interconnections are wire bonding and flip-chip techniques. Wire bonding is a relatively cheap and rapid interconnection option, yet it is often prone to sway upon encapsulant molding and high parasitic inductance, often requiring external or on-chip passive components for compensation at mm-wave frequencies [1]. Flip-chip techniques reduce interconnection length and parasitics yet suffer from high sensitivity to coefficient of thermal expansion (CTE) mismatch as well as circuit detuning from the close proximity to on-package signal routing below the bumped IC [2].

Inkjet and 3D printing technologies allow for the selective deposition of electronic materials in a 3D fashion, where dielectric and metallic patterns can be fabricated directly onto virtually any host to create fully-printed, vertically-integrated electronic systems and packages [3-5].

Specifically from a wireless perspective, inkjet printing offers the advantage of incorporating printed interconnects and multilayer antenna structures with wireless dies and packages in an efficient SoP scenario [6, 7]. The continued study of the materials and processes behind these additive printing techniques allows for the integration and innovation of advanced fabrication methods to realize emerging wireless system designs specifically within the mm-wave regime [8-10].

This paper outlines the utilization of inkjet and 3D printing processes to provide fundamental solutions to the growing field of wireless mm-wave packaging. Fully inkjet-printed 3D interconnects are presented for directly interfacing IC dies with a packaging substrate. Stereolithography (SLA) 3D printing processes are outlined targeting two standard resin classifications, including ceramic-loaded resins for low CTE and high permittivity packages. These processes are applied to the realization of 3D-printed IC encapsulations with application-specific functionality, including the integration of dielectric lenses and frequency selective surface (FSS)-based filters. Finally, inkjet and 3D printing processes are combined to realize sloped mm-wave interconnects for the fabrication of through-mold vias (TMVs), highlighting the functionality of interconnecting an IC die with the other planes of the IC package in a truly 3D fashion.

II. Printing Materials and Processes

As with traditional fabrication technologies, the materials involved with additive printing methods must adhere to specific rheological, mechanical, and electrical constraints in order to ensure maximum functionality in a practical production environment. Specifically, the materials used within inkjet printing with standard piezoelectric dispensing methods must exhibit a low viscosity (< 30 cP) and small differential from the surface energy of the host substrate (typically within 10 mN/m) [11]. The viscosity and surface tension of the inks play major roles in jetting characteristics (voltage, temperature, waveform) and ink wetting, respectively. SLA 3D printing involves the selective photonic exposure and crosslinking of a UV-photosensitive material in a consecutive layer-by-layer fashion to realize a homogenous 3D object. The general process flow outlining SLA printing is shown in Fig. 1. Whereas the feature size of inkjet printing is determined by drop volume and ink spreading on a surface, the resolution of an SLA printing system is determined in the *Z*-axis by the build plate stepper motor and in the *XY*-plane by the source of maskless UV exposure system. The exposure source for an SLA system is typically either laser-based or based on digital light processing (DLP) technology, where *XY*-feature resolution is determined by laser spot size or pixel width at a certain focal length, respectively.

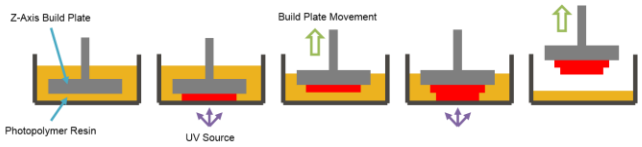

Fig. 1. Stereolithography (SLA) 3D printing process diagram.

A. *Inkjet Printing*

Inkjet printing is performed using a Dimatix DMP-2831 printing platform with 10 pL cartridges. Two ink materials are printed to realize 3D multilayer electronic structures: a silver nanoparticle-based ink and a polymer-based dielectric ink. Metallic features are fabricated using Sun Chemical EMD-5730, a silver nanoparticle-based ink with 40 wt% silver content loading. After patterns with this ink are printed, low temperature sintering (< 200 °C) occurs to yield a conductivity approximately one fifth of bulk silver [12]. Passivating films and 3D ramp structures are fabricated with a Microchem SU-8 polymer-based ink. The thickness of these printed dielectric films depends on the number of printed layers or cartridge passes, which can vary from 4 µm to beyond 100 µm [11]. Curing the SU-8 ink is a three-step process. First the samples are baked on a hot plate from 60–110 °C over 10 min. Then UV crosslinking is performed with a thickness-dependent exposure. Finally, the samples are baked at 100 °C for 7 min to complete the dielectric pattern processing.

B. *Stereolithography (SLA) 3D Printing*

Two SLA photoresins are outlined for this effort, both formulated to cure at near-UV wavelengths between 350–410 nm: Vorex (orange color) from MadeSolid and Porcelite from Tethon3D. Vorex is an acrylate-based resin optimized for mechanical resilience, highlighting impact strength and toughness. Porcelite is a crystalline silica particle-loaded resin with the ability to realize fully-ceramic objects when fired near 1000 °C. However, high-temperature firing is typically not ideal for back end of line (BEOL) packaging processes, so in this case the inclusion of ceramic composites in the resins are highlighted for a potential increase in permittivity and reduction of coefficient of thermal expansion (CTE) due to the nature of the dispersed ceramic particles.

The 3D structures in this effort are printed using a custom LittleRP SLA 3D printer with a Viewsonic PJD7828HD DLP projector with a 1080p resolution operating as a 3000 lm maskless UV source. The projector is focused at a set distance from the vat of resin and target printing site to provide a resolution of approximately 40 µm in the *XY*-plane based on the size of a single pixel. Printed layer thickness, or *Z*-axis resolution, is varied depending on the desired structure and process time with a minimum of 10 µm per layer. To facilitate delicate sample handling, a

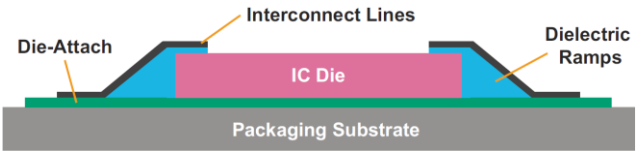

Fig. 2. Cross-section of inkjet-printed 3D interconnects. [7]

1 mm thick glass slide is affixed to the steel build plate using a photopolymer adhesive, allowing for easy removal of the sample from the printing system with minimal force while preserving the adherence of the sample to the build plate. The exposure time of each consecutive layer depends on the layer thickness and requires tuning to avoid under- and overexposure. For this effort, 50 µm layers of the Vorex and Porcelite resins are exposed for 3 and 6 seconds, respectively. A layer thickness of 10 µm is used with the Vorex material requiring a per-layer exposure time of 1 sec. After the SLA printing is completed, the samples are submerged and agitated within two consecutive isopropyl alcohol (IPA) baths to clean off any residual unexposed resin material. To complete the SLA process, a final post-print 1 J/cm^2 UV exposure is performed to ensure that the 3D-printed Vorex and Porcelite samples are fully cured.

III. Inkjet-Printed 3D Interconnects

The design of the printed 3D interconnects is comprised of the following elements shown in Fig. 2: an IC die, a packaging substrate, a die attach material, dielectric ramp structures, and coplanar waveguide (CPW) transmission lines [7]. For this work, a blank 2×2.7 mm silicon die with a thickness of 50 µm and a bulk resistivity of 10 Ω-cm is used as a proof-of-concept prototype for mm-wave transceiver dies. The packaging substrate is chosen to be a 1 mm-thick glass slide to facilitate handling throughout the fabrication process, however this technology could be applied to other more commonly-used packaging substrates, including metallic, flexible organic, and ceramic hosts.

Fabrication of the 3D interconnect samples begins with the patterning of the die attach material on a bare glass slide using a Dimatix DMP-2831 inkjet printer. Three layers of the SU-8 polymer ink are printed and then undergo a soft bake. A silicon die is then manually placed onto the die attach, followed by the remainder of the SU-8 ink curing profile: a 250 mJ/cm^2 exposure of 365 nm ultraviolet (UV) light and a 100 °C bake for 7 min. With the die attached, dielectric ramps are printed with SU-8 ink to transition between the die and the substrate. The ramp structures are patterned to extend approximately 400 µm onto the surface of the die and 800 µm onto the substrate. The purpose of extending the pattern onto the surface of the die is to allow for a uniform ramp to be realized with the minimum number of printed layers, where adhesion of the ramp to the top of the die is improved when material is deposited onto

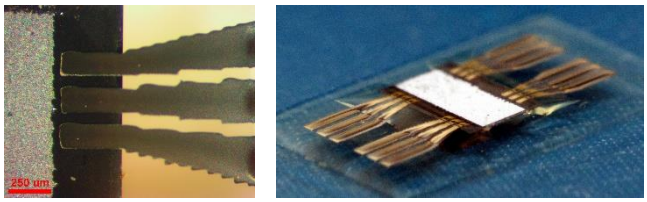

(a) (b)

Fig. 3. Inkjet-printed 3D interconnects with die: (a) micrograph and (b) perspective view.

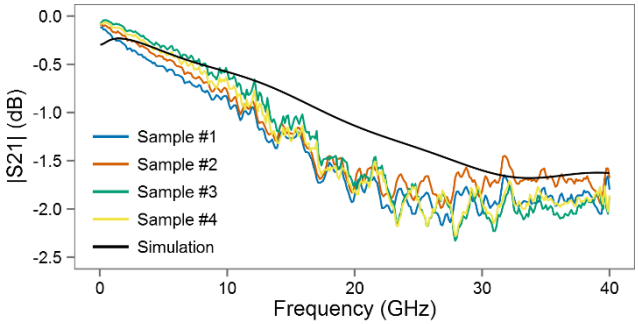

Fig. 4. Insertion loss simulation and measurements of inkjet-printed 3D interconnects. [7]

both the die and the packaging substrate instead of the substrate alone due to the rheological nature of the polymer ink. Additionally, the extension of the material onto the die allows for increased adhesion of the printed interconnects to the unpolished surface of the dummy die. Five layers of the SU-8 polymer ink are printed to pattern the ramps, followed by the standard curing profile with the substitution of a 300 mJ/cm^2 UV light exposure to account for the thicker dielectric ramps. Fabrication is concluded with the printing of the CPW transmission line traces using silver nanoparticle ink. Before printing, the sample undergoes a 30 sec exposure to UV ozone (O_3) to optimize the surface energy of the printed ramps and substrate for the wetting of the Cabot CCI-300 silver nanoparticle ink. Three layers of the silver nanoparticle ink are printed, followed by oven sintering at 180 °C for 1 hr.

Images of the printed 3D CPW interconnect samples are shown in Fig. 3. The staggering effect present in the fan-out of the traces is due to the 20 µm resolution of the CPW line pattern. The key dimensions of the printed CPW interconnects exhibit on average less than ± 3% variation across the four printed samples. High frequency simulations of the CPW interconnect prototypes are conducted using CST Microwave Studio. The S-parameters of the printed interconnect samples are measured with an Anritsu 37369A VNA utilizing 250 µm pitch ground-signal-ground (GSG) probes from Cascade Microtech. Measured and simulated insertion loss parameters from 0.04–40 GHz are presented in Fig. 4, yielding an insertion loss of 0.6–0.8 dB/mm at 40 GHz. Deviations from the simulated characteristics are

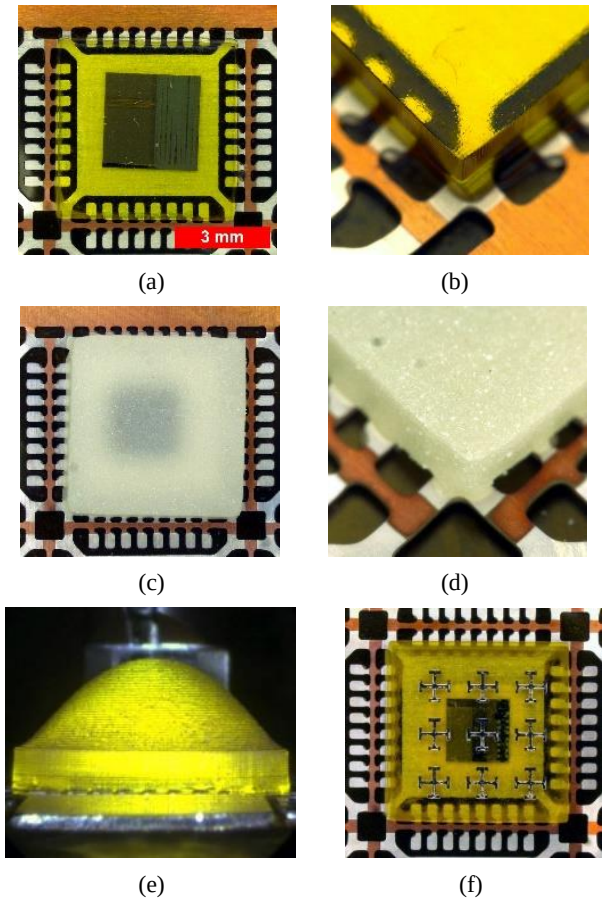

Fig. 5. 3D SLA-printed die encapsulations on a metallic QFN leadframe: Vorex encapsulation (a) top view and (b) perspective detail view; Porcelite encapsulation (c) top view and (d) perspective detail view; (e) Vorex dielectric lens structure; (f) Vorex encapsulation with inkjet-printed FSS. [13]

likely the result of the morphology of the dielectric ramp structures, a feature that is difficult to precisely model in simulation. Return loss of the printed lines is measured to be less than -10 dB across the measured frequency span, exhibiting acceptable matching for low-loss mm-wave interconnection.

IV. 3D-Printed IC Encapsulation

Additive printing technologies are emerging as an efficient means to fabricate robust 3D packages for microelectronic systems. The flexible nature of these technologies are highlighted, where a full line of designs for die attach, interconnects, and encapsulation can be realized with significantly reduced tooling costs and complexity. In [3], Lopes et al. combine SLA and direct write printing methods to realize a 3D package for a timer circuit using an LM555 timer. Cavities and sloped vias are included in the printed package to allow for chip embedding and multilayer integration, respectively, however the feature size of the metallic interconnects is not adequate for interfacing with IC dies. In another recent effort, Merkle et al. demonstrate the development of multichip modules (MCMs) for D-band (110–170 GHz) wireless applications using polymer spin-coating and layer-by-layer masking for encapsulation along with physical vapor deposition (PVD) for interconnect metallization [4]. This process offers lithography-level feature sizes for interconnects and structures, however issues of large tooling time and cost are present due to the nature of lithographic processes.

The printing of an IC die encapsulation using the above outlined SLA materials is presented with the goal of replacing standard epoxy molding and stamping methods of package encapsulation [13]. In addition to being an ambient-pressure room-temperature fabrication process, SLA printing allows for the realization of selectively-patterned and nontraditionally-shaped encapsulation solutions, while simultaneously maintaining tan δ within the same range of standard epoxy molding compound materials [14].

Silicon dies with 280 µm thickness and areas of 2×2 mm and 3×3 mm are attached to a metallic QFN leadframe using an inkjet-printed polymer-based ink. After the dies are attached, 5.5×5.5×1 mm encapsulations are printed directly onto the leadframe-attached dies using the Vorex and Porcelite materials with the outlined processing conditions. This is accomplished by affixing the QFN leadframes to the build plate of the SLA printer in order to directly pattern the die encapsulations onto the leadframes. Fig. 5 presents images of the printed Vorex and Procelite encapsulations. In addition to the standard encapsulation, an SLA printing tool can be configured to fabricate nontraditional encapsulation shapes, for example open cavities for microelectromechanical systems (MEMS) sensors and dielectric lenses for package-integrated antennas, presented in Fig. 5(e). These novel package shapes can be achieved by simply changing the 3D model in the SLA printing tool, highlighting the reconfigurable nature of this technology for diverse application-specific packaging applications.

This newly demonstrated SLA printing technology for packaging can be easily combined with existing inkjet printing technology to realize the post-process fabrication of on-package components, including passive components, antennas, sensors, and periodic FSS structures. Fig. 5(f) presents an FSS structure inkjet-printed directly onto a 3D-printed encapsulation using a Dimatix DMP-2831 inkjet printing system and silver nanoparticle-based ink for such applications as wireless filtering, shielding, and aperture-coupled component integration.

V. On-Package Printed Sloped Interconnects

With the ability to inkjet print electronic structures directly onto a 3D-printed encapsulation, interest is placed

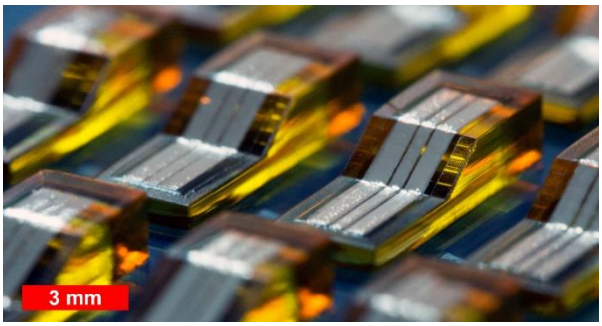

(a)

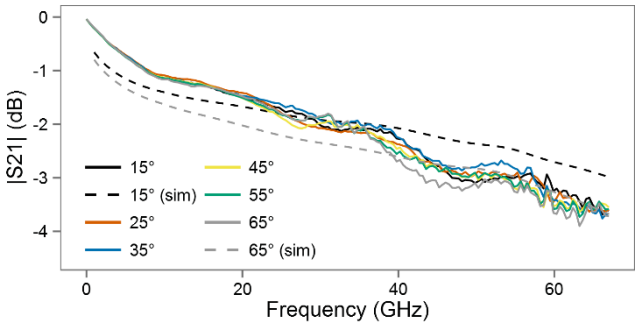

(b)

Fig. 6. (a) 3D-printed ramp structures with inkjet-printed CPW interconnects, highlighting the 35° slope ramps. (b) |S21| insertion loss measurements and simulations of printed CPW TMVs with varying slope. [13]

onto how these structures can interface with a molded IC within the package. The concept of directly interconnecting a molded IC die to an external plane of its encapsulation is an area not widely investigated in literature. Amkor Technology Inc. (Chandler, AZ, USA) demonstrates a through-mold-via (TMV) process for low-profile package-on-package (PoP) integration, however interconnects are limited to solder balls typically used with ball grid array (BGA) packages [15]. Due to the interest in SoP design solutions for mm-wave wireless systems, efficient TMV interconnects in the mm-wave regime are desired to expand the possibilities of system integration.

The integration of inkjet printing with 3D printing technology requires an analysis of the capabilities of this typically 2/2.5D technology in truly 3D applications. In order to evaluate the integration of SLA 3D printing and inkjet printing technologies for mm-wave packaging, ramped interconnect structures with slopes ranging from 15–75° are characterized with the Vorex SLA material [13]. Sample Vorex ramps measuring 3×7.5 mm with a 1 mm tall ramp and 10 µm layer height resolution are fabricated with a LittleRP SLA printer to represent the sloped walls of a partial IC encapsulation. Next, two layers of a MicroChem SU-8 polymer-based ink are printed onto the ramp structure in order to passivate the 10 µm layer steps of the 3D-printed ramps with a film thickness of approximately 8–12 µm. Sun

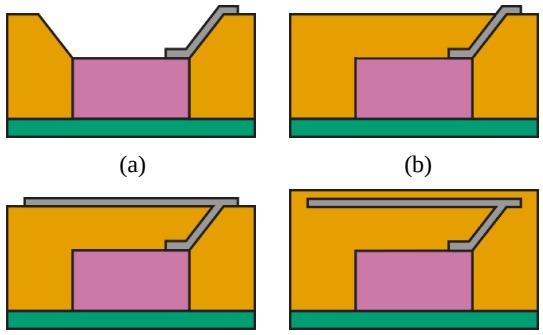

Fig. 7. Process flow outline of TMV integration with in-package structures: (a) partial encapsulation (orange) 3D-printed onto IC die (pink) and packaging substrate (green) with inkjet-printed sloped interconnects (grey), (b) encapsulation fill 3D-printed to seal package, (c) multilayer antenna/passive/etc. topology inkjet-printed onto encapsulation surface, (d) final encapsulation 3D-printed to finalize package.

Chemical EMD5730 silver nanoparticle-based ink is printed to pattern coplanar waveguide (CPW) interconnect lines from the die-level to the encapsulation-level of the ramp structures. Finally, the printed ramp interconnects are sintered in an oven at 150 °C for 1 hr to complete the fabrication process. Fig. 6(a) shows a perspective micrograph of the test vehicle containing multiple samples of the SLA ramps with varying slope. The insertion loss of the printed TMV interconnects is characterized up to 67 GHz with an Agilent E8361C PNA and 67A-GSG-250-C probes from GGB, presented in Fig. 6(b) aside Ansys HFSS simulations for the two extreme cases (15° and 65°). All slopes ranging from 15–65° exhibit an insertion loss between 0.5–0.6 dB/mm at 60 GHz, where the 75° slope did not achieve complete electrical connectivity. The printed 3D interconnects presented in this paper yield a 10× reduction in insertion loss from standard wirebond interconnects at 60 GHz [16].

The proposed process flow of TMV fabrication and package-integrated structure realization is outlined in the schematics of Fig. 7. Fabrication begins with the inkjet printing of TMV interconnects directly onto the pads of the IC, leading up the slope of the 3D-printed partial encapsulation to the top plane of the encapsulation. Next, 3D printing is used to seal the partial encapsulation, leaving the inkjet-printed interconnects exposed at the new top plane of the encapsulation. Multilayer antenna array and/or passive components are then inkjet printed directly onto the encapsulation, interfacing with the TMVs leading up from the die. Finally, 3D printing is used to seal the wireless package. This combination of inkjet and 3D printing technologies enables the realization of highly-integrated 3D SoP designs in a low-cost, highly reconfigurable and scalable fashion to create intelligent wireless packages.

VI. Conclusion

This paper outlines the utilization of fully-additive inkjet and 3D printing technologies to fabricate 3D mm-wave interconnects and packages. CPW transmission lines are employed to interconnect an IC die with a packaging substrate, exhibiting suitable insertion and return loss for mm-wave systems. The processing and material characteristics of two 3D-printed SLA materials are also presented for various packaging applications: including printed die encapsulation along with use as an RF substrate for on-package antenna arrays, lenses, and periodic FSS structures. Finally, inkjet-printed CPW transmission lines are combined with 3D-printed ramp structures with slopes ranging from 15–65° for use as mm-wave TMV interconnects characterized up to 67 GHz. The SoP integration of 3D and inkjet printing technologies has the potential to enable the realization of fully-printed arbitrarily-shaped "smart" wireless packages for such emerging applications as automotive radar and 5G mobile communication.

Acknowledgment

The authors would like to acknowledge the National Science Foundation (NSF), Defense Treat Reduction Agency (DTRA), Semiconductor Research Corporation (SRC), and Texas Instruments (TI) for this support with these efforts.

References

[1] Y. P. Zhang and D. Liu, "Antenna-on-Chip and Antenna-in-Package Solutions to Highly Integrated Millimeter-Wave Devices for Wireless Communications," *IEEE Transactions on Antennas and Propagation*, vol. 57, pp. 2830-2841, 2009.

[2] A. Jentzsch and W. Heinrich, "Theory and measurements of flip-chip interconnects for frequencies up to 100 GHz," *IEEE Transactions on Microwave Theory and Techniques*, vol. 49, pp. 871-878, 2001.

[3] A. Joe Lopes, E. MacDonald, and R. B. Wicker, "Integrating stereolithography and direct print technologies for 3D structural electronics fabrication," *Rapid Prototyping Journal*, vol. 18, pp. 129-143, 2012.

[4] T. Merkle, R. Götzen, J.-Y. Choi, and S. Koch, "Polymer multichip module process using 3-D printing technologies for D-band applications," *IEEE Transactions on Microwave Theory and Techniques*, vol. 63, pp. 481-493, 2015.

[5] S. A. Nauroze, J. G. Hester, B. K. Tehrani, W. Su, J. Bito, R. Bahr, *et al.*, "Additively Manufactured RF Components and Modules: Toward Empowering the Birth of Cost-Efficient Dense and Ubiquitous IoT Implementations," *Proceedings of the IEEE*, vol. 105, pp. 702-722, 2017.

[6] B. K. Tehrani, B. S. Cook, and M. M. Tentzeris, "Post-process fabrication of multilayer mm-wave on-package antennas with inkjet printing," in *Antennas and Propagation & USNC/URSI National Radio Science Meeting, 2015 IEEE International Symposium on*, 2015, pp. 607-608.

[7] B. K. Tehrani, B. S. Cook, and M. M. Tentzeris, "Inkjet-printed 3D interconnects for millimeter-wave system-on-package solutions," in *Microwave Symposium (IMS), 2016 IEEE MTT-S International*, 2016, pp. 1-4.

[8] Y. Arbaoui, V. Laur, A. Maalouf, and P. Queffelec, "3D printing for microwave: Materials characterization and application in the field of absorbers," in *Microwave Symposium (IMS), 2015 IEEE MTT-S International*, 2015, pp. 1-3.

[9] P. I. Deffenbaugh, R. C. Rumpf, and K. H. Church, "Broadband microwave frequency characterization of 3-D printed materials," *IEEE Transactions on Components, Packaging and Manufacturing Technology*, vol. 3, pp. 2147-2155, 2013.

[10] A. L. Vera-López, E. A. Rojas-Nastrucci, M. Córdoba-Erazo, T. Weller, and J. Papapolymerou, "Ka-band characterization and RF design of acrynolitrile butadiene styrene (ABS)," in *Microwave Symposium (IMS), 2015 IEEE MTT-S International*, 2015, pp. 1-4.

[11] B. K. Tehrani, C. Mariotti, B. S. Cook, L. Roselli, and M. M. Tentzeris, "Development, characterization, and processing of thin and thick inkjet-printed dielectric films," *Organic Electronics*, vol. 29, pp. 135-141, 2016.

[12] B. S. Cook and A. Shamim, "Inkjet printing of novel wideband and high gain antennas on low-cost paper substrate," *IEEE Transactions on Antennas and Propagation*, vol. 60, pp. 4148-4156, 2012.

[13] B. K. Tehrani, R. A. Bahr, W. Su, B. S. Cook, and M. M. Tentzeris, "E-band characterization of 3D-printed dielectrics for fully-printed millimeter-wave wireless system packaging," in *Microwave Symposium (IMS), 2017 IEEE MTT-S International*, 2017.

[14] L. Li, A. Kapur, and K. B. Heames, "Characterization of transfer molding effects on RF performance of power amplifier module," in *Electronic Components and Technology Conference, 2004. Proceedings. 54th*, 2004, pp. 1671-1677.

[15] A. Yoshida, S. Wen, W. Lin, J. Kim, and K. Ishibashi, "A study on an Ultra Thin PoP using through mold via technology," in *Electronic Components and Technology Conference (ECTC), 2011 IEEE 61st*, 2011, pp. 1547-1551.

[16] T. Krems, W. Haydl, H. Massler, and J. Rudiger, "Millimeter-wave performance of chip interconnections using wire bonding and flip chip," in *Microwave Symposium Digest, 1996., IEEE MTT-S International*, 1996, pp. 247-250.